ACERP: Vol. 1, No. 3, (Autumn 2015) 1-10

Advanced Ceramics Progress

Research Article

Journal Homepage: www.acerp.ir

# Investigation of crystallization and sinterability properties of $BaO-SiO_2-Al_2O_3$ glass-ceramics containing $K_2O$ and $B_2O_3$

**N. Aniseh, M. Rezvani*, H. Ghahremanzadeh ,S. Tabean**

*Department of Ceramic, Materials and Energy Research Center, Karaj, Iran*

*PAPER INFO*

***Paper history:***
**Received** 03 December 2014
**Accepted in revised form** 02 November 2015

*Keywords*:
Sinterability
Hexacelsian
Celsian
SOFC

*ABSTRACT*

$BaO-SiO_2-Al_2O_3$ glass-ceramics containing $K_2O$ and $B_2O_3$ were prepared using conventional melting of batch powered, quenching in water and crystallization of sintered glass. XRD patterns presented hexacelsian and celsian as two major crystallized phases. Introducing $K_2O$ improved crystallization of hexacelsianmore than $B_2O_3$.Glass-ceramic structure are studied using FTIR. Inspecting the property of sintered samples of 4% wt $K_2O$ + 4% wt $B_2O_3$ and 2% wt $B_2O_3$ amount of additives. Furthermore condensation temperature reduced up to 850ºC. Glass-ceramics containing 4% wt. $K_2O$ + 4%wt.$B_2O_3$ exhibited more sinterability in comparison with 2%wt $B_2O_3$ samples. SEM micrograph of glass-ceramic intersections with metallic alloy and electrolyte depicted the connections characteristics.

## 1. INTRODUCTION

Investigations for new energy sources have led to foundation of secondary energy plants. Among all, fuel cells are able to directly produce electric energy in required ranges. Due to various requirements several types of fuel cells are developed. Concerning to electrolyte type, fuel cells are categorized in 5 groups. In comparison to all others Solid Oxide Fuel Cells, SOFC, has various advantages such as: compatibility with environment, variety of suitable fuels, high efficiency, and being economical. Problems caused by corrosion are reduced by ceramic electrolytes. While, their high working temperature (800-1000ºC) causes incompatibility between fuel cells elements. SOFCs are consist of 4 main parts: electrodes, electrolyte, interconnect and sealing. Sealing is used to separate fuel gases from oxidant in working temperature of SOFCs [1-3]. Working conditions of SOFCs which sealing should tolerate are:

- Over 750ºC working temperature.
- Oxidizing and reducing environments of anode and cathode, respectively.
- Oxygen partial pressure varies in the range of $1\times10^{-13}$ to $2\times10^{4}$ Pa.
- Permissible life time 10000 hours (5 year).

Majority of the research done on SOFC`s sealing are focused on rigid bond sealing. Various kind of glass sealing are developed which is waxed in temperatures above SOFC`s working temperatures and seals using physical and chemical bonds. while cooling these bonds down to SOFC`s working temperature they crystallize and produces completely rigid sealing condition. The main advantages of such sealing is its capability to use various glasses to obtain the optimize cells physical properties such as heat transfer coefficient [1].
Other specifications of sealing are [1]:

- Any chemical reaction between the sealing and its neighboring parts is not allowable; i.e. it should have steady bonds in oxidizing and reducing atmosphere.
- Viscosity should be $10^5$ Pa-s at connecting temperature (1000ºC) and $>10^9$ in working condition (850ºC).
- Minimum difference of expansion coefficients with other Cell component (TEC=$7\text{-}11\times10^{-7}K^{-1}$)

Since glass-ceramics can meet most of the above mentioned requirements, they are considered as an ideal sealant [2].
In the current work $BaO-SiO_2-Al_2O_3$ glass-ceramic system was chosen. $K_2O$ and $B_2O_3$added to the system

*Corresponding Author's Email: m_rezvani@tabrizu.ac.ir

as flux and their effect on crystalizing temperature, sintering and glass structure are studied. [1, 4, and 9-12] This system creates two principle phases, monocelsian and hexacelsian [5,9, and 10]. The structure of barium aluminosilicate glasses is consist of $(Al,Si)O_4$ tetrahedral. These elements are coincident from corners. Ba cations are located in the vacancies between the tetrahedrals. Crystalizing barium aluminosilicate creation of hexacelsian and monocelsian phases are possible [4- 6].

Hexacelsian phase ($BaAl_2Si_2O_8$) has needle shape and hexagonal structure, while celsian inincludes monoclinic structure. Hexacelsian has more open structure in comparison with monocelsian, therefore it has higher thermal expansion coefficient ($8\times10^{-6}1/°C$ ) than celsian ($2.29\times10^{-6}1/°C$), which is order of metals expansion coefficient thusshows better sealant properties. More ever the phase has better compatibility with the remained glass matrix. So hexacelsian crystallization is important in the system. Heat treating the glasses, first the hexacelsian phase crystalize. Increasing heat treating temperature celsian phase also began to crystalize. Fortunately converting hexacelsian to mono celsian is very slow. This is the key point in using this glass-ceramics as sealant element. [7, 8]

Since formation zone of hexacelsian in the triple diagram of $BaO\text{-}Al_2O_3\text{-}SiO_2$ is very narrow and it has high formation temperature, decreasing the crystallization temperature of hexacelsian is very important.

A lot of researchers have worked on this and related systems [3-8]. Eichler et al. studied crystallization properties of BAS systems in SOFC sealants at 1999 [5].

Nonstoichiometric celsian glass-ceramics with $BaO.2SiO_2$-50wt%$Ba.Al_2O_3.2SiO_2$50% ($B_2S$-$BA_2S$) chemical combination are studied by Sung et al. 2000 [12 and 13]. Sohn et al. studied chemical and thermal compatibility of BAS system using YSZ electrolyte at 2004 [9]. BCAS glasses are studied by S.Ghosh in 2008 [14].

$Ba_2SiO_3$ phase may also crystalizeduring crystallization process. Existing $Ba_2SiO_3$, leads to increases thermal expansion coefficient inglass-ceramics containing barium [6, 13, and 15-18].

## 2. EXPERIMENTAL PROCEDURES

$BaO\text{-}SiO_2\text{-}Al_2O_3$ with hexacelsian stoichiometric composition (13.5%wt $Al_2O_3$, 23.275%wt $SiO_2$ and 63.22%wt BaO) was chosen as the base composition. Theoretically, at melting temperatureof 1370ºC, glass forms only 48.1%wt hexacelsian, which is because of high formation temperature and narrow area of hexacelsian in trinary phase diagram. Therefore melting temperature held at 1450ºC to ensure formation of hexacelsian phase.

4% wt.$K_2O$ with 4% wt.$B_2O_3$ was added to the base composition which showed completely pourable molten glass. At the next stage $B_2O_3$content was reduced to 2% and the evacuation of molten glass was still complete. Selection of $B_2O_3$ was based on literaturein system of $BaO\text{-}SiO_2\text{-}Al_2O_3$ [5,13, 19-21].

Table 1. represents chemical composition of glass including various amounts of additives.

**Table 1.** Chemical compositionof glass containing various amounts of additive (%wt)

| Sample | $K_2O$ | $B_2O_3$ | $Al_2O_3$ | BaO | $SiO_2$ |
|---|---|---|---|---|---|
| H8 | 8 | 0 | 13.50 | 63.22 | 23.27 |
| H4B4K | 4 | 4 | 13.50 | 63.22 | 23.27 |
| H2B | 0 | 2 | 13.50 | 63.22 | 23.27 |

Where, H represents Hexacelsian phase.Glasses were prepared by conventional melting process. All of raw materials were used in high purity grades (higher than 99wt.%), as follow: $Al_2O_3$ ($Al_2O_3$Merck no.234745) BaO ($BaCO_3$ by Merck no. 101077) $B_2O_3$ ($B_2CO_3$ by Merckno. 100162) $K_2O$($K_2CO_3$Merckno. 310263) SiO2 (Hamedan,acid washed). Glass frits were prepared by melting of the raw materials at 1450°C for 1h in alumina crucible and quenched in cold water. Frits were dried and milled to particle size <63 μm. Thermal properties of glass powders were determined by Differential Thermal Analysis (DTA-Linseis L181) at a heating rate of 10°C $min^{-1}$. Frits mixed with 5% wt. % polyvinyl alcohol solution and then pressed axially 30 MPa into a pellet with 22mm diameter and 4mm thickness. The bulk density of sintered glass-ceramics were measured usingArchimedes methods (ASTM C373-88). Glass-ceramics powder density were determined using pycnometery method (ASTM D2320-98). Study of glass-ceramics structuralcomposition is done by FTIR instrument (Tensor27, braker, German) Crystalline phase precipitated during sintering was determined by X-Ray Diffraction (XRD) analysis (Siemens, model D-500).

Considering XRD patterns and using equation (1) content of glass-ceramic crystalline phase can be calculated [22].

$$\text{Crystalline phase (\%)} = \frac{I_g - I_x}{I_g - I_b} \quad (1)$$

Where:

$I_b$: maximum peak intensity in mechanical mixture of components

$I_g$: maximum peak intensity of the amorphous glass

$I_x$: maximum peak intensity of the crystallized sample.

Samples crystal size, in the crystalline material, obtained using X-ray diffraction patterns and equation (2), Debye-Scherer equation, is given as [23]:

$$D = \frac{K\lambda}{\beta_{1/2}\cos\theta} \quad (2)$$

Where:
D: crystal size (in ˚A order)
K: constant equal to 0.9
λ: wavelength of incident X –ray beam. For Cu cathode tube equal to 1.54056 ˚A
θ: angles corresponding to peaks in X-ray diffraction pattern
$\beta_{1/2}$ is root square and defines as:

$$\beta_{1/2} = (Bm^2 - bs^2)^{1/2}$$

Where, Bm is the diffraction peak width at half height for sample, and bs is the diffraction peak width at half height of standard sample.
Lattice constant of hexacelsian crystals obtained using equation (3) [24]:

$$d_{hkl} = \frac{1}{\sqrt{\frac{4}{3a^2}(h^2 + k^2 + l^2) + {l^2}/{c^2}}} \quad (3)$$

Where a and c are lattice constants, while h, k, and l are miller indices of planes, and $d_{hkl}$ is distance between planes with mentioned indices. Main difficulty of this approach for obtaining lattice constants is change of lattice constant through different planes.
In calculating lattice constant, displacement of X-Ray peaks should be noted. Also practically tip of the peaks don't indicate the actual location of maximum intensity. There are different corrections for this error, best approach seems to assume location of peak at half or higher heights of peak [22]. To correct this error, Riley Nelson function define as:

$$F(\theta) = \frac{1}{2}\left[\frac{\cos^2(\theta)}{\sin(\theta)} + \frac{\cos^2(\theta)}{\theta}\right] \quad (4)$$

Where θ is Bragg angle.
In this method when Riley Nelson function approaches to zero ($F(\theta) \to 0$) value of lattice constant can be calculated [22].
Values of a and c can be obtained by equation (3), Nelson Reilly equation determine F(θ) values. Using obtained values, plot of F(θ) vs. lattice constants can be sketched. By extrapolation of the line -which fits sketched plot- to vertical axis (lattice constant axis) lattice constants can be calculated [22].
In this study lattice parameters have approximate values, neglecting F(θ).
Microstructure of glass and glass-ceramics were characterized by Field Emission Scanning Electron Microscopy (FE-SEM-Mira Tescan). The glass-ceramics were polished and etched in 5%wt. HF solution and subsequently were coated by a thin film of gold for 30 seconds.
In order to simulate the sealant function in SOFCs, pellets of base glass is prepared and pre sintering process is done in 800 °C. Connection is done by sandwiching glass pellets between metallic alloy (croffer22APU) and $ZrO_2$ body and applying load and heat up to 1000°C by rate of 10 °C /min then sating one hour in the temperature. Also in order to analyzing the connection 950°C with the staying time of 4 hours is used for better crystallization of glass-ceramic. At the end reducing the temperature to the working temperature of SOFCs, 850°C and staying time of 50 hours to simulate the working condition of SOFCs.

## 3. RESULT AND DISCUSSION

### 3.1. Thermal analysis by DTA

DTA results for H2B and H4B4K samples are shown in Figure 1(a). Since H8 composition was not melt in this temperature, it was omitted in this study.
Alkaline metals such as $K_2O$ usually reduces glasses bond strength.Introducing this component to base material acts as a suitable flux and reduces viscosity drastically. Moreover $K_2O$ (assuming a as atomic distance, z as atomic number and $Z/a^2$) has poor ionic field strength ($K^+$ 0.12). According to the DTA results, H2B sample showed higher $T_g$ rather than H4B4K sample. Increasing $B_2O_3$ enhance viscosity and $[BO_3]$ groups in the structure. In H4B4K samples, the content of $K_2O$ was not enough to alter the coordination number of boron from 3 to 4. Also $K_2O$ content wasn't enough to decrease viscosity of the glass and integrity of structure, therefore $T_g$ didn't change.
The structure of H4B4K samples are more open because of $[BO_3]$ groups, as they have a higher content of non-bridging oxygenin comparison with H2B samples. This issue facilitates atomic diffusion and make crystallization of the glass more feasible at lower temperatures. This phenomena is proved in the FTIR results. Therefore, the H4B4K samples shows lower $T_c$ in comparison with H2B samples.
Fiqure 1(b) represents dilatometre results for H4B4K and H2B glasses.
Figure (1) (a) DTA analysis (b) Percent of linear change vs. temperature of H4B4K and H2B glasses.

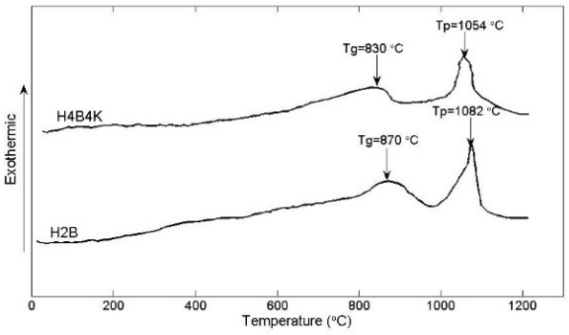


**Figure 1a.**

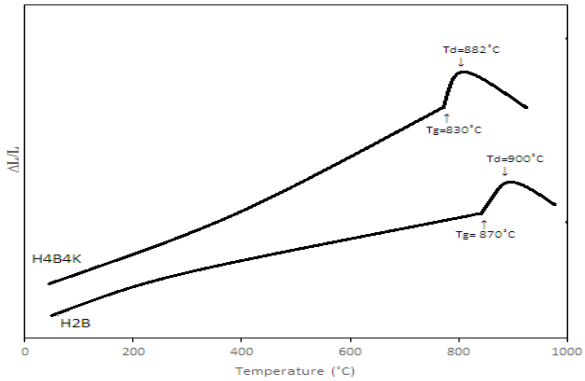


**Figure 1b.**

## 3.2 STRUCTURAL ANALYSES BY FTIR

According to FTIR patters in alkaline alominosilicate glasses in the case of H2B and H4B4K sample patterns following items can be concluded:The band allocated in 480.35cm$^{-1}$ is because of nonsymmetrical bending vibration of Si-O-Si. Aluminum is allocated in tetrahedral location in glass structure. If a tiny amount of Al is locate in octahedral location the related band is allocated in 500cm$^{-1}$. Because of strong bonds of Si-O-Si in [$SiO_4$] absorption of [$AlO_6$] is covered by [$SiO_4$] [25].

The band allocates in 691.15cm$^{-1}$ is caused by capacity vibration of Al-O in [$AlO_4$] tetrahedral. When Al and Si magnitude is equal this band is possible to be from vibration of Al-O in [$AlO_4$] and Si-O in [$SiO_4$] at the same time. Also bending vibration of B-O-B in trigonal [$BO_3$] is also allocates in this location so distinguishing the band is from which is difficult [26].

The band allocated in 966.48cm$^{-1}$ is because of tensile vibration of [$BO_4$] structure. Because of high amount of BaO this band can be caused by non-bridging oxygen in the structure. Also a huge amount of $(AlO_6)^{3+}$ is existed in the molten structure which can rupture the 3d structure of molten and increases amount of non-bridging oxygen[25].

The band allocates in 1056.36 cm$^{-1}$ is because of tensile vibration of Si-O in the [$SiO_4$] tetrahedral and also vibration of B-O in the tetrahedral of [$BO_4$][25]. Bands allocates in 1392.23 cm$^{-1}$ is because of tensile vibration of B-O in [$BO_3$] structure. This band is [$BO_3$] group characteristics [26].

In the FTIR patterns of H4B4K there is no distinct deference with the patterns obtained from H2B samples. The only distinguishable deference is the band which is allocates in 1205.8cm$^{-1}$. This band is caused by the tensile vibration of boroxy ring. Also by increasing $B_2O_3$ and introducing $K_2O$ to the glass structure the band allocates in 1389.71cm$^{-1}$ is increased and the intensity of the band in 1054.36cm$^{-1}$ decreases. Increase in band intensity located in 1389.1cm$^{-1}$ is means increase in [$BO_3$] groups in system and decrease in the peak intensity in cm$^{-1}$ is because of decreasing [$BO_3$] groups. Increasing the peak intensity declares that $B_2O_3$ first introduces as [$BO_3$] but in more amount part of it converts to [$BO_4$] and boroxy ring.

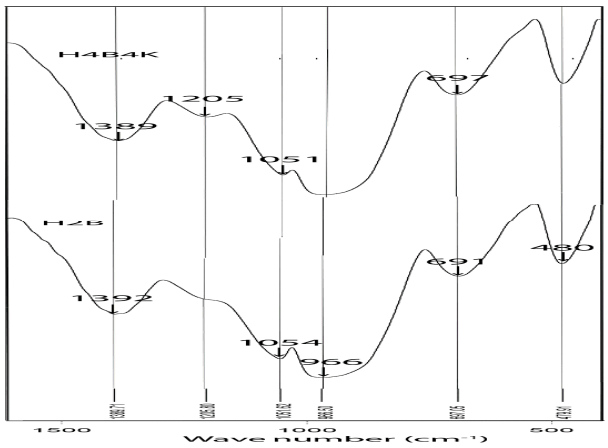


**Figure 2**. FTIR results for H2B and H4B4K.

## 3.3. CRYSTALLINE BEHAVIOR

In order to perform a phase study of the frit glass and crystallized composition, X-ray Diffraction patterns (XRD) employed. According to Figure (1) heat treatment performed at temperatures above 900ºC (after glass transition temperature) with 100ºC intervals. XRD patterns of frit and heat treated glasses for 1 hour at different temperatures are shown in Figure (3) and (4). Figure (3) depicts XRD patterns of glass with H2B composition.

In 900ºC patterns shows presence of $BaAl_2Si_2O_8$, merely. Content of crystallized glass is negligible. Similarly at 1000ºC the crystallized phase is hexacelsian and another phases were not formed.

Increase of heat treating temperature amplifies peak intensities. At 1100ºC there are other peaks along with

hexacelsian peaks. This peaks corresponds to the $BaSiO_3$ phase (first peak appear at 2θ=26.22º).

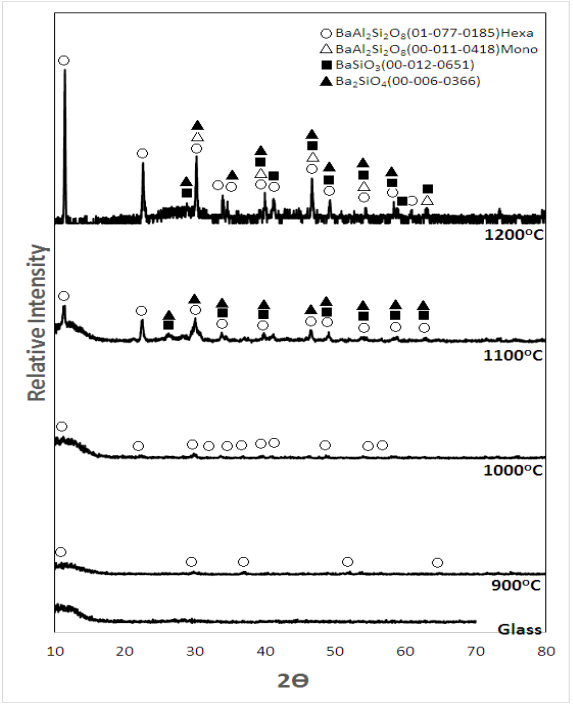


**Figure 3.** XRD patterns of H2B frit and heat treated glasses for 1 hour at different temperatures.

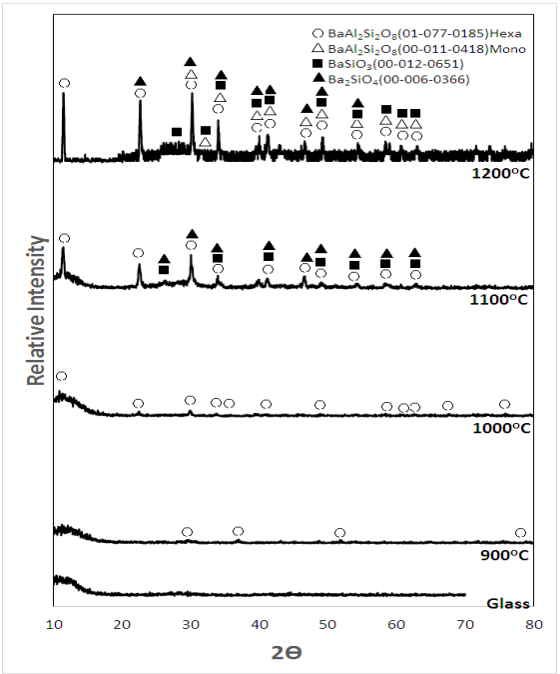


**Figure 4** XRD patterns of H4B4K frit and heat treated glasses for 1 hour at different temperatures.

In the glass-ceramic structure, hexacelsian phase was observed as the major phase, at all heat treating temperatures.

XRD patterns of H4B4K composition are shown in Figure (4). There is no detectable peak infrit of this composition. At 900ºC glass is amorphous. By increasing heat treating temperature up to 1000ºC, weak peaks of hexacelsian are observable. As it is obvious first peak appears in 2θ=11.49˚.

At 1100ºC,as well as hexacelsian phase, $BaSiO_3$ and $Ba_2SiO_4$ were formed. First peak of $BaSiO_3$ and $Ba_2SiO_4$ overlap at 2θ=26.22 .At 1200ºC hexacelsian, $Ba_8Al_2O_{11}$ and $BaSiO_3$ phases are observable in glass-ceramic, by the way predominant phase in H4B4K sample is hexacelsian.

As seen in XRD patterns, hexacelsian incline to form in all compositions and its content increases with increasing temperature. In 1200ºC, celsian phase crystallized in monoclinic structure.

As major phase in the glass-ceramics is hexacelsian, calculated crystalline phases can be assumed asthis phase merely. Crystalized phase was calculated using equation 1. Content of the crystalline phase vs. temperature is shown in Figure (5). The crystalline phase increases with increasing heat treating temperature. Below specific temperature (1100ºC) approximate crystalline phase content in the H4B4K sample is greater, comparing with H2B sample.

Crystalline phase increases with increase in heat treating temperature. In case of H4B4K, there is no substantial change crystalline phase content between 1100ºC and 1200ºC.

In order to explain DTA results, it can be said, effect of added $B_2O_3$ on viscosity at high temperatures is much less than its effect at low temperatures. As a result, at temperatures between 1100ºC and 1200ºC viscosity didn't change so much, thus content of crystalline phase almost remains constant with its value at 1100ºC [27].

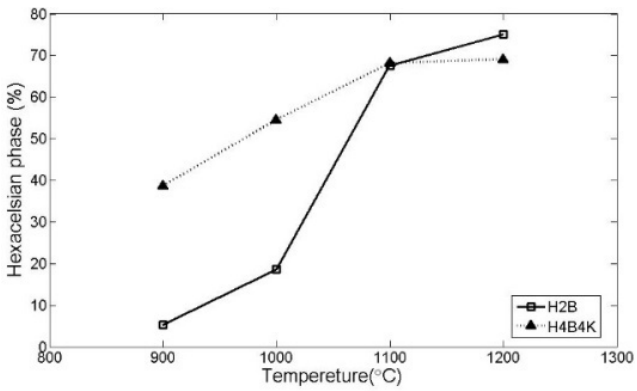


**Figure 5.** content of the hexacelsianphase vs. temperature.

Crystallite size are obtained using equation 2. Crystal size variation vs. temperature for both H4B4K and H2B samples are shown in Figure (6).

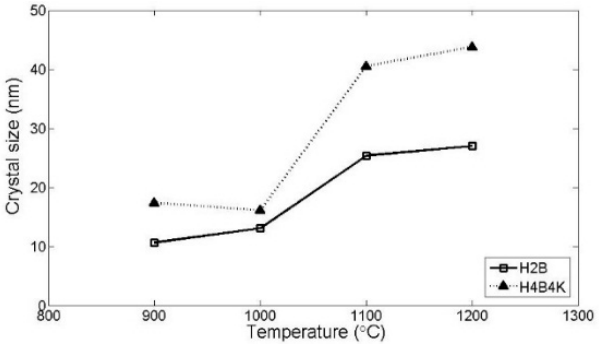


**Figure 6.** Variation of crystalline particle size vs. temperature, for both samples: H4B4K and H2B.

Lattice parameters are calculated using equation 3. Figure (7) shows variation of lattice constant, a and c versus temperature for H4B4K and H2B samples.

Thermal expansion coefficient of a glass depends on glass structure symmetry, In other words buckling of bonds in glass structure effects thermal expansion coefficient. For instance, this parameter has value of $0.6\times10^{-6}1/ºC^{-1}$ and $14.4\times10^{-6}1/ºC^{-1}$for $SiO_2$ and $B_2O_3$ respectively.

Modifiers in silicate glasses produce non-bridging oxygen which can reduce symmetry of glass structure and results in increase of thermal expansion coefficient [48].

Due to higher content of modifiers in the H4B4K samples, amount of non-bridging oxygen is higher in this structure. H4B4K has lower structural symmetry so it has more open structure than H2B and atomic penetration is performed easily, thus percentage of crystalized phase in H4B4K sample is more than H2B sample. Lattice parameters in H4B4K samples are greater than H2B samples. Due to lower structural symmetry, H4B4K has bigger linear expansion than H2B.

### 3.4. SINTERABILITY OF H2B AND H4B4K GLASS-CERAMICS

In order to study sinterability of H2B and H4B4K glass-ceramics, glass powder (with average particle diameter<63 μm) pressed into pellet with 22mm diameter and 5mm thickness through 30 MPa uniaxial compression stress.

Samples heat treated for an hour at different temperatures varying from 850˚C to 1000˚C, with intervals of 50˚C.

Due to floatability of amorphous phase at temperatures above $T_g$, sintering of Glass powder begins around

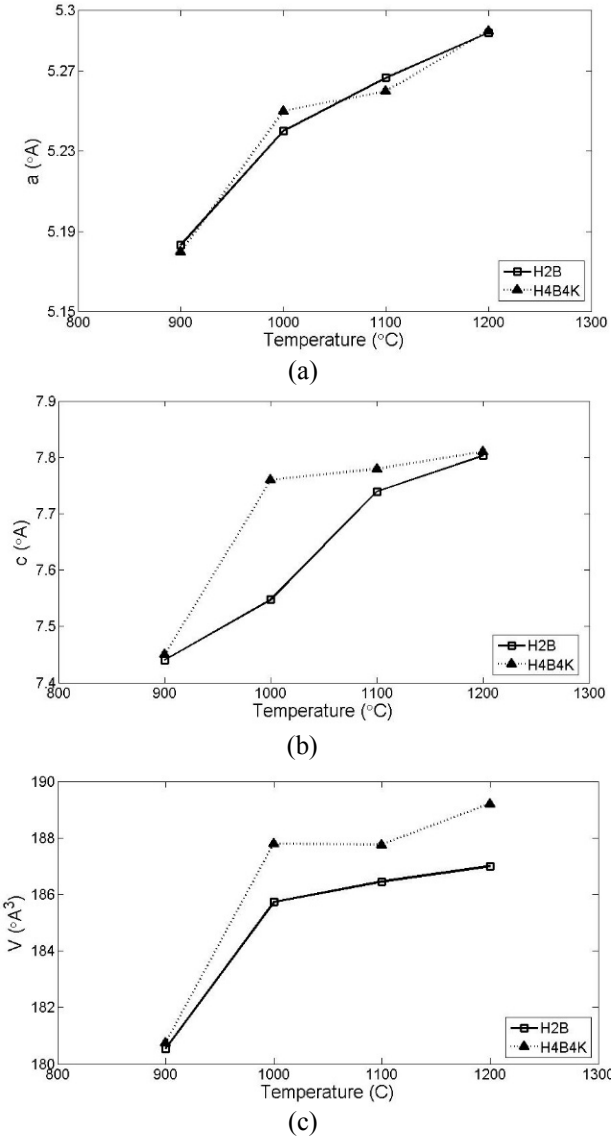


**Figure 7.** Variation of lattice constant of (a) a,(b) c axes, and (c) the variation of unit cell volume for H4B4K and H2B samples.

850˚C and continue till 950˚C. Linear expansion and viscosity of samples are shown in the Figure 8. As temperature increases, penetration of the ions in to the ceramics structure increases, so porosity decreases and density increases, Further increase in temperature, above 950ºC leads to formation of hexacelsian phase as predominant phase (as seen in the Figure 4), thus decrease in linear expansion and relative condensed phase, as shown in Figure(8).

Sintering can be defined as increase in relative density of sample, as initial porosities seem to disappear through diffusive procedures. Mechanical and physical properties of the porous sample usually heals up sharply during sintering process.

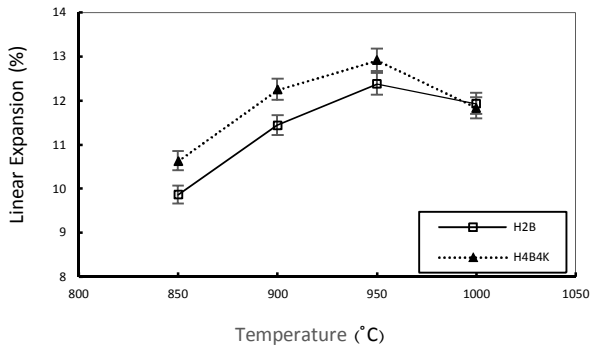


(a)

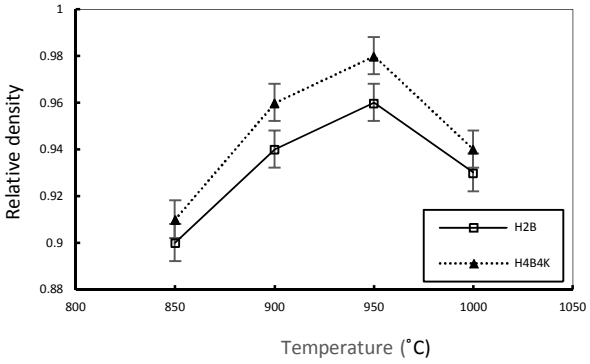


(b)

**Figure 8.** (a) Linear expansion, and (b) Relative density of glass-ceramics vs.temperature.

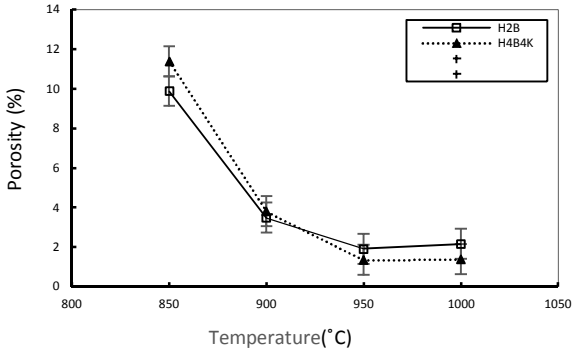


(a)

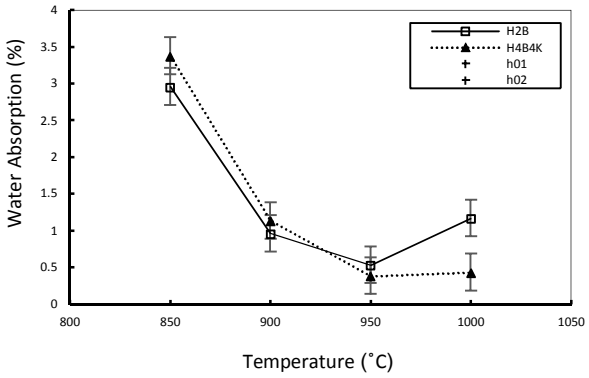


(b)

**Figure 9.** (a) porosity percentage (b) water absorptionvs. temperature for sintered glass-ceramics.

Unlike metals, polymers and intermetallic compounds which casting and hot/cold forming are considered aspossible forming methods, in the case of condensed ceramics the main forming process is sintering [29].
Water absorption and openporosity proportion for sintered glass-ceramics are shown in Figure (9).
During the heat treatment, there are two paths for reducing free energy of system, viscose flow and crystallization. These two phenomena have mutual and competitive effect on reducing free energy of system [29].
If crystallization occurs prior to condensation, viscosity of the residual glass increases, which subsequently reduces viscose flow. Crystallization decreases bulk and grain boundary diffusion which results in a porous structure [20, 30].
Due to higher content of $B_2O_3$ in H4B4K comparing to H2B, H4B4K sample shows higher relative density and lower porosity.
Better viscous flow amplifies linear expansion rate and sinterability. Due to higher H4B4K density, it has a lower water absorption and porosity percentage in comparison with H2B.

## 3.5. INVESTIGATION OF MICROSTRUCTURE BY SEM METHOD

SEM image of H4B4K heat treated in 900 °C for 1 hour is shown in Figure 10. It is clear that the glass-ceramic very little crystalize in the temperature. According to XRD results it can be declare that the white dotes is hexacelsian phase in the glass amorphousmatrix.

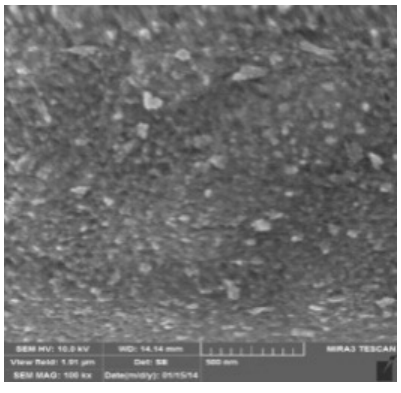

**Figure 10.** SEM image of H4B4K heat treated in 900°C for 1 hour with 100000X magnification.

SEM image of H4B4K heat treated in 1100°C for 1 hour is shown in Figure 11. It is been seen that increasing heat treating temperature is led to increase crystalize phase content in the glass matrix. According to XRD results the crystalized phase is consist of hexacelsian, $Ba_2SiO_4$ and $BaSiO_3$.

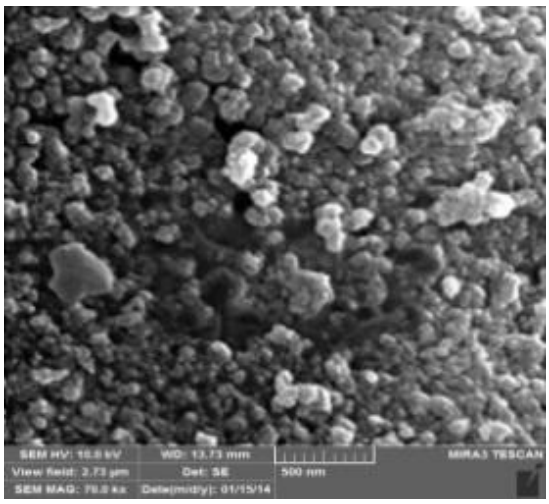

**Figure 11**. SEM image of H4B4K heat treated in 1100°C for 1 hour with 70000 magnification.

According to XRD, DTA, and sintering results, H4B4K was chosen as a sealing glass. Morphology of chromium containing alloy (croffer22APU) – glass-ceramic– $ZrO_2$ cross section was investigated by SEM.
SEM image of intersection of $ZrO_2$-H4B4K connection is shown in Figure 12. Interconnection layer has condense and compressed structure, as seen in the Figure. Several cracks are seen in the electrolyte which caused by incompatibility of thermal expansion. In the cracks border different structure can be detected which is surface melting of glass paste and penetrating into the cracks of electrolyte. Magnified image of the prompted area in the Figure 12(a) is shown in the Figure 12(b).
Unlike the electrolyte– sealant connection section, alloy– sealant glass connection is completely homogeneous with no cracks. Glass surface melt and penetrate to alloy crevasses. Glass penetration into the metal structure is negligible. Non connection of glass to the alloy is easily seen in the more magnifying images.
SEM image of section of chromium alloy – sealant glass connection is shown in Figure 13.

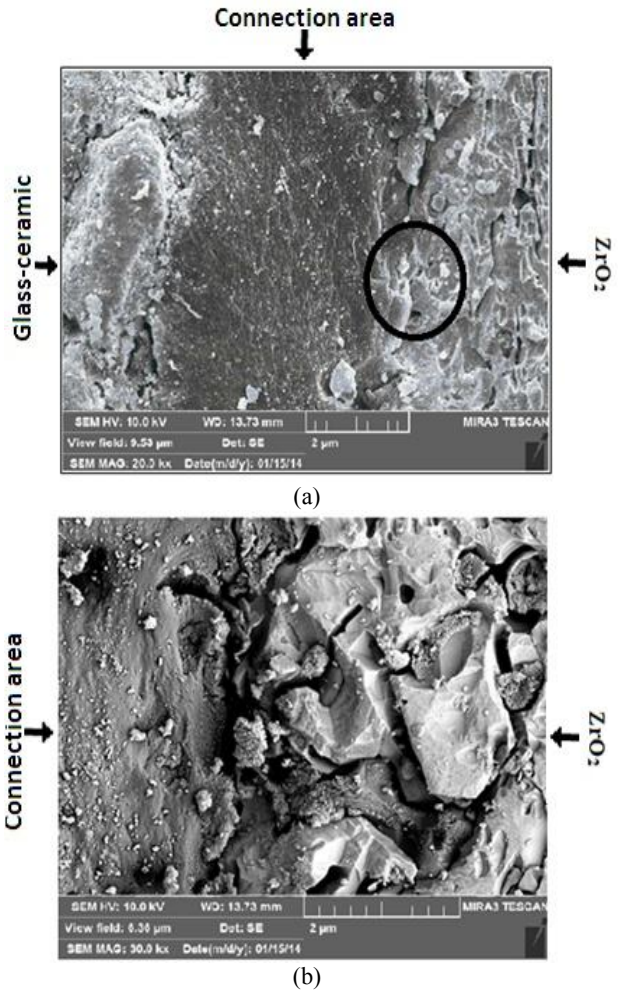


**Figure 12.** SEM image of section of $ZrO_2$-H4B4K connection (a) 20000X (b) 30000X magnification.

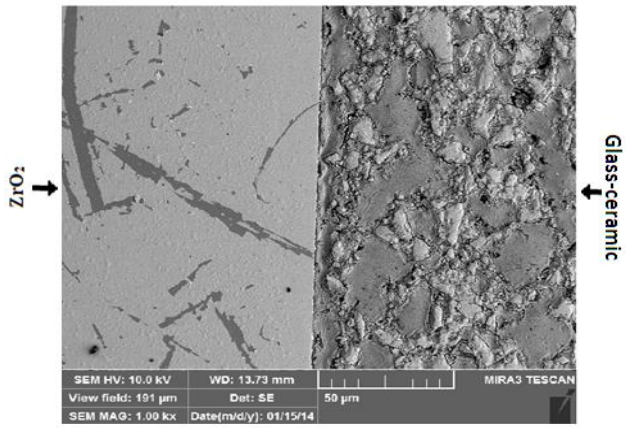


**Figure 13.** SEM image of intersection of chromium alloy – sealant glass connection with 1000X magnification.

## 4. CONCLUSION

1- According to DTA results glass-ceramics containing 2%wt. $B_2O_3$ have higher $T_g$ and $T_p$, in comparison with H4H4K samples. Introducing $B_2O_3$ leads to increase in viscosity and [$BO_3$] in the structure. This phenomena is confirmed in the FTIR results as well. In H4B4K sample $K_2O$ contents is not enough to increase coordination number of boron from 3 to 4 and decrease viscosity, lattice stability and increase Tg. More open structure of H4B4K is caused by [BO3] group and higher amount of non-bridging oxygen. This fact facilitate atomic penetration, so crystallization occurs in lower temperature in comparison with H2B sample. Thus, $T_c$ in H4B4K is lower than H2B sample.

2- Relative density in H4B4K is higher than H2B sample. Increase in $B_2O_3$ increases lattice fracture and increases fluidity, i.e. the glass easily flowed and make it possible to reach higher densities. Higher linear expansion interpreted better sinterability because of viscos flow. Higher compression of H4B4K rather than H2B, leads to lower water absorption and porosity in comparison with H2B.

3- Regarding to XRD, sintering, and DTA, H4B4K was chosen as the sealant.

4- Concerning to SEM results of connection area of $ZrO_2$-glass-ceramic, in the electrolyte zone cracks caused by incompatibility of heat expansion coefficient is shown. But surface melting of glass and glass penetration into electrolyte cracks leads the connection take place.

In the SEM images of glass-ceramic- chromium alloy no cracks caused by incompatibility is detected glass molten and penetrates in the alloy crevasses in small amount. Penetration of glass into the alloy is negligible, so no good connection is done between elements.

## REFERENCES


1. Arora, Anu, Kulvir Singh, and O. P. Pandey. "Thermal, structural and crystallization kinetics of $SiO_2$-BaO-ZnO-$B_2O_3$-$Al_2O_3$ glass samples as a sealant for SOFC.*" International journal of hydrogen energy* "36, no. 22 (2011): 14948-14955.
2. Sun, Tao, Hanning Xiao, Wenming Guo, and Xiucheng Hong. Effect of $Al_2O_3$ content on BaO-$Al_2O_3$-$B_2O_3$-$SiO_2$ glass sealant for solid oxide fuel cell. "***Ceramics international*** 36, no. 2 (2010): 821-826.
3. Sung-Bum Sohn and Se-Young Choi, Gyeung-Ho Kim, Hue-Sup Song, and Goo-Dae Kim, Suitable Glass-Ceramic Sealant for Planar Solid-Oxide Fuel Cells, ***J. Am. Ceram. Soc***., 87 [2] 254–60 (2004).
4. Sohn, Sung-Bum, Se-Young Choi, Gyeung-Ho Kim, Hue-Sup Song, and Goo-Dae Kim. "Suitable Glass-Ceramic Sealant for Planar Solid-Oxide Fuel Cells. ***Journal of the American Ceramic Society*** 87, no. 2 (2004): 254-260.
5. S. B. Sohn, et al, ***J.Non Cryst.Solids.*** 297 (2002) 103.
6. Eichler, K., G. Solow, P. Otschik, and W. Schaffrath. "BAS ($BaO.Al_2O_3.SiO_2$)- glasses for high temperature applications. ***Journal of the European Ceramic Society*** 19, no. 6 (1999): 1101-1104.
7. C. H. Drummond III and N. P. Bansal, Crystallization and Properties of Sr-Ba Aluminosilicate Glass-Ceramic Matrices ***Ceram. Eng. Sci. Proc***. 11 (1990) 1072.
8. M. J. Hyatt, N. P. Bansal, Crystal Growth kinetics in $BaOAI_2O_32SiO2$ and $SrOAI_2O_32SiO_2$ Glasses, ***J. Mater. Sci***. 31 (1996) 172 184
9. Dai, Zhou, Jian Pu, Dong Yan, Bo Chi, and Li Jian. "Thermal cycle stability of $Al_2O_3$-based compressive seals for planar intermediate temperature solid oxide fuel cells. ***International Journal of Hydrogen Energy*** 36, no. 4 (2011): 3131-3137.
10. Smeacetto, Federico, A. Chrysanthou, Milena Salvo, T. Moskalewicz, F. D'Herin Bytner, Lakshmi Chandru Ajitdoss, and Monica Ferraris. "Thermal cycling and ageing of a glass-ceramic sealant for planar SOFCs. ***International Journal of Hydrogen Energy*** 36, no. 18 (2011): 11895-11903.
11. ***Ceramic-review*** Article: reseant advances in metal– ceramic brazing : www.Scielo.br-scielo.php
12. Lahl, N., K. Singh, L. Singheiser, K. Hilpert, and D. Bahadur. "Crystallisation kinetics in AO-$Al_2O_3$-$SiO_2$-$B_2O_3$ glasses (A= Ba, Ca, Mg). ***Journal of Materials science*** 35, no. 12 (2000): 3089-3096.
13. Yang, Zhenguo, Jeff W. Stevenson, and Kerry D. Meinhardt. "Chemical interactions of barium–calcium–aluminosilicate-based sealing glasses with oxidation resistant alloys. ***Solid State Ionics*** 160, no. 3 (2003): 213-225.
14. Nicholas, M. G. "Joining Structural Ceramics" In Designing Interfaces for Technological Applications, edited by S. D. Peteves, ***Elsevier Applied Science,*** (1989): 49-76.
15. Yang, Zhenguo, Kerry D. Meinhardt, and Jeff W. Stevenson. "Chemical compatibility of barium-calcium-aluminosilicate-based sealing glasses with the ferritic stainless steel interconnect in SOFCs. ***Journal of the Electrochemical Society*** 150, no. 8 (2003): A1095-A1101.
16. Touloukian, Yeram Sarkis. "Thermophysical Properties of High Temperature Solid Materials." Volume 4. "Oxides and Their Solutions and Mixtures". Part I. "Simple Oxygen Compounds and Their Mixtures. ***The MacMillan*** Co., NewYork (1966).
17. Chou, Yeong-Shyung, and Jeffry W. Stevenson. "Long-term thermal cycling of Phlogopite mica-based compressive seals for solid oxide fuel cells. ***Journal of power sources*** 140, no. 2 (2005): 340-345.
18. Holand, Wolfram, and George H. Beall. "Glass-ceramic technology. ***The American Ceramic Society***, Westerville, OH, (2002).
19. Bansal, Narottam P., and Mark J. Hyatt. "Crystallization kinetics of BaO–$Al_2O_3$–$SiO_2$ glasses. ***Journal of Materials Research*** 4, no. 05 (1989): 1257-1265.
20. Yi- Ju Chen, W. C. W. "The Suitability of BaO-$B_2O_3$-$Al_2O_3$ Glass System Used as Sealant for SOFC. ***Institute of Material Science.***
21. Aboutaleb, Djamila, Brahim Safi, Azzeddine Ayadi, and Aicha Iratni. "Effect of the $Al_2O_3$ and BaO Addition on the Thermal and Physical Properties of Trinary Glass System ($B_2O_3$-BaO-$Al_2O_3$). ***Journal of Materials Science and Engineering*** B 3 (5) (2013): 291-295.
22. S. Manafi, and A. Soltanmoradi, investigation of sintered hydroxide apatite nano-powers , ***Modern processes in Material***, no 3, (1391).
23. M. Sadighi, and Reza Nazem zadeh, investigation the effect of peak determining method on ,***Airo space mechanics***, volume7, no2 (1390): 73-88.
24. H. Lipson, "The Study of Metals and alloys by X-ray Powder Diffraction" , Published for the ***International Union of Crystallography by University College Cardiff Press Cardiff, Wales***.(2001).

25. Bimalendu N. Roy, infrared Spectroscopy of Lead and Alkaline-Earth Aluminosilicate glasses, ***J. Am. Son***.73[4]846-55(1990)
26. Tao Sun Haning, et. al. Effect of Al2O3 contant on BaO-Al2O3-B2O3-SiO2 Glass sealant for Solid Oxide Fuel Cell, ***Ceramics International*** 36(2010)821-826.
27. Li, H. C., D. G. Wang, J. H. Hu, and C. Z. Chen. "Effect of the partial substitution of $K_2O$, MgO, $B_2O_3$ for CaO on crystallization, structure and properties of $Na_2O–CaO–SiO_2–P_2O_5$ system glass-ceramics. ***Materials Letters*** 106, (2013): 373-376.
28. Prasanta Kumar-Ojha, "Physical and Thermal behaviuor of Sr-La-B-Si Based SOFC glases. ***Journal of Power sources***, 196 (2011): 4594-4598 .
29. Bengisu, Murat, ed. "Engineering ceramics. ***Springer***, (2001).
30. Goel, Ashutosh, Dilshat U. Tulyaganov, Anna Maria Ferrari, Essam R. Shaaban, Andreas Prange, Federica Bondioli, and José MF Ferreira. "Structure, Sintering, and Crystallization Kinetics of Alkaline-Earth Aluminosilicate Glass–Ceramic Sealants for Solid Oxide Fuel Cells. ***Journal of the American Ceramic Society*** 93, no. 3 (2010): 830-837.